# A Feasibility Study for Signal-in-Space Design for LEO-PNT Solutions With Miniaturized Satellites

Ruben Morales Ferre, *Student Member, IEEE*, Jaan Praks, *Senior Member, IEEE*,
Gonzalo Seco-Granados, *Senior Member, IEEE*, and Elena Simona Lohan, *Senior Member, IEEE*

*Abstract*—The global navigation satellite systems (GNSSs) are increasingly suffering from interferences, such as coming from jammers and spoofers, and their performance is still modest in challenging urban and indoor scenarios. Therefore, there are efforts worldwide to develop complementary positioning, navigation, and timing (PNT) solutions. One such complementary method under current research is the so-called LEO-PNT, namely, PNT solutions based on low-Earth orbit (LEO) satellites, and in particular on small-sized or miniaturized satellites. Such satellites have low-to-moderate costs of building, launching, and maintenance. Several challenges are to be overcome when designing a new LEO-PNT solution, concerning all three satellite segments: 1) the signal-in-space (SIS) or space segment; 2) the ground segment; and 3) the user/receiver segment. This article presents a survey of the SIS design challenges under the inherent constraints of wireless-channel propagation impairments as well as some design recommendations for SIS features. We address different constellation types, achievable coverage limits, and geometric dilution of precision (GDOP) bounds, as well as achievable carrier-to-noise ratios (CNRs) under a realistic wireless channel model, based on a MATLAB Quadriga simulator. We also discuss several optimization criteria regarding LEO-PNT SIS design, by taking into account the tradeoff between a low cost/low number of satellites in orbit on the one hand, and a sufficient coverage and good CNR for PNT purposes on the other hand.

Ruben Morales Ferre and Elena Simona Lohan are with the Electrical Engineering Unit, Tampere University, 33720 Tampere, Finland (e-mail: ruben.moralesferre@tuni.fi; elena-simona.lohan@tuni.fi).

Jaan Praks is with the Department of Electronics and Nanoengineering, Aalto University, 02150 Espoo, Finland (e-mail: jaan.praks@aalto.fi).

Gonzalo Seco-Granados is with the Systems Telecommunications Department, Universitat Autònoma de Barcelona, 08193 Barcelona, Spain (e-mail: gonzalo.seco@uab.cat).

## I. Introduction

THE FUTURE sky will host tens of thousands of satellites in various orbits, ranging from low-Earth orbits (LEOs) to medium-Earth orbits (MEOs) and geo-stationary orbits (GEOs). One of the main research and development interests nowadays in the wireless world is toward LEO orbits [1], [2], [3], [4]. LEO orbital altitudes are between about 200 and 2000 km above the Earth, mostly below the Van-Allen radiation belts, making less costly to build and launch satellites in these orbits than at MEO/GEO altitudes of 20 000–36 000 km, which are inside the outer Van-Allen radiation belts. For this reason, MEO satellites need radiation-hardened components, which can be 100–1000 times more expensive than small-satellite commercial off-the-shelf (COTS) components at LEO altitudes. Another trend related to satellite design is the miniaturization, namely, the trend to go toward smaller and more compact satellite dimensions, in order to provide low-cost low-power solutions [5].

A well-adopted classification based on satellite mass is shown in Table I, together with examples of satellite systems (in the sky or under development) belonging to each category. The four global navigation satellite systems (GNSSs), namely, Galileo, GPS, GLONASS, and BeiDou, are also listed among the examples, as they will represent the benchmark for any future LEO-PNT solution [6], [7]. Currently, the attosat and zeptosat categories are only in the research phase, without any commercially available satellite system.

The most used classes of miniaturized satellites nowadays, according to [8], are micro- and nano-classes, encompassing more than 50% of existing small satellites. Small satellites are operating in LEO orbits, which are the focus of this article. In some papers, the microsats and nanosats are referred to, together, as *CubeSats*,[1] because the CubeSat

---

[1]In some research papers, CubeSat terminology is strictly used for nanosats and picosats.

TABLE I
SATELLITE CLASSIFICATION WITH RESPECT TO SATELLITE MASS AND ORBITAL ALTITUDE

| Typical Orbits | Satellite Class | Mass [kg] | Examples of satellite systems for communication or positioning purposes |
|---|---|---|---|
| MEO, GEO | Large sats | >= 1000 | GPS, Beidou, Glonass, Boeing 702, O3B mPower, Telestat Telstar 19V, Thales Alenia Leosat, Ziyuan 3 |
| | Medium sats | 500-1000 | Galileo, Iridium/Iridium NEXT, Telestat LEO satellites, |
| LEO | Minisats | 100-500 | SpaceX Starlink, OneWeb, Amazon Kuiper, Hongyun, Facebook Athena, Xona Space, GeeSpace |
| | Microsats | 10-100 | Iceye, Capella Space, BlackSky Global, Kepler Communications LEO sats, Hellas-Sat, Tekever |
| | Nanosats | 1-10 | PlanetLabs Dove/SuperDove CubeSats, Spire Global Lemur-2 and Minas, Myriota, UWE-4, Xiaoxiang-1, Tyvak nanosats, DICE CubeSats, QuakeSat, NanoAvionics, Hiber, Kleos space CubeSat , Horizon Technologies Amber |
| | Picosats | 0.1-1 | Swarm Technologies SpaceBEE, Gauss PocketQubes, Alba Orbital Unicorn, Fossa Systems (FossaSat) |
| | Femtosats | 0.01-0.1 | SunCube FemtoSat |
| | Attosats | 0.001-0.01 | N/A |
| | Zeptosats | 0.0001-0.001 | |

standard is a most common form factor for current nano- and micro-satellites. Typically, the mass of a small satellite beyond 500 kg is defined in the CubeSats unit (U), under the form of 1U CubeSat, 2U CubeSat, etc. The reference CubeSat unit is a cube-sized satellite of dimensions $10 \times 10 \times 10$ cm$^3$. Thousands of such miniaturized satellites are already in the sky and thousands more of them are planned to be launched in the next 2–5 years, targeting applications such as broadband connectivity, Earth observation, IoT, environmental monitoring, air traffic management, etc. [5], [9], [10]. The geolocation applications via LEO satellites, or the so-called LEO-PNT solutions [11], [12], are still in a very incipient phase. Some of the small-satellite/CubeSats systems, which have had some research developments regarding LEO-PNT capabilities, are Kleos Space,[2] Hiber, Horizon Technologies Amber, XonaSpace, GeeSpace, and Skycraft Foundation; however, public information regarding these systems and their positioning capability is still limited.

To the best of our knowledge, surveys on LEO-PNT solutions and their design challenges for signal-in-space (SIS) design are still lacking in the current literature. The goal of this article is to summarize, in a compact manner, the design challenges for SIS of LEO-PNT solutions under wireless channel path-loss propagation constraints, overview potential solutions, and present concrete examples and optimization criteria toward the choices of the SIS design. The main contributions of this article are as follows.

1) Presenting a comprehensive survey of SIS design challenges for LEO-PNT solutions relying on miniaturized satellites.
2) Analyzing the optimal constellation patterns under the minimum number of satellites for a good tradeoff between low cost and global coverage targets.
3) Presenting concrete link-budget calculation examples as well as the carrier-to-noise ratio ($C/N_0$) and geometric

dilution of precision (GDOP) characterization and discussing their significance in SIS design.
4) Offering a road-map ahead with still-to-be-solved challenges and potential solutions toward future robust SIS design for LEO-PNT systems as well as preliminary SIS design parameters regarding number and altitudes of the satellites, constellation type, orbital inclinations, and carrier frequencies.

## II. RELATED WORK

A survey on CubeSats has been recently provided in [8], but the authors focused only on communications aspects via LEO CubeSats, and positioning aspects were not addressed at all. Another comprehensive survey on CubeSats has been recently published in [13]. Again, positioning based on LEO signals was outside the scope of that survey, but the authors addressed topics such as the existing frequency bands in use for current CubeSat systems, the impact of constellation type on the communication-link performance, modulation and coding schemes, medium access control, and networking layer design. This article is complementary to the works in [8] and [13], as we focus on the wireless positioning capabilities of the CubeSat systems, which were not a part of the above-mentioned studies.

LEO-PNT concepts have been addressed previously in [11], [12], and our previous work in [6]. Related works addressing the parts of the SIS design for LEO satellites are, for example, in [14], [15], [16], and [17]. Savitri *et al.* [14] implemented a semi-analytical approach to find an optimal constellation design. The results in there were only valid for a specific region (South Korea) and no optimal global coverage was analyzed. Zong and Kohani [15] optimized a Walker constellation for global coverage by means of genetic algorithms. Ge *et al.* [16] and Guan *et al.* [17] proposed optimal Walker constellations for GNSS purposes, but not at LEO orbits. Ge *et al.* [16] analyzed few aspects of LEO constellations, such as the number of LEO orbital planes, the number of LEO satellites, and the selection of orbital inclinations. After analyzing
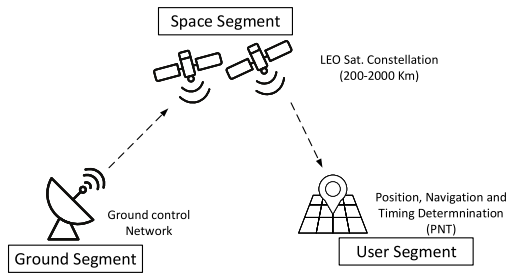
[2]http://kleos.space/commercial/

Fig. 1. Three-segment architecture of any satellite system.

different options, Ge *et al.* [16] proposed an optimal constellation with 240 LEO satellites and three orbital inclinations at 90°, 60°, and 35°, respectively. The results in [17] showed that a much larger and complex constellation than studied in [16] is needed for global and optimal coverage for PNT purposes. The optimal constellation proposed in [17] is composed of near-polar Walker orbits with a total of 1284 satellites distributed on 6 orbits, 100 km apart, between 900 and 1500 km altitudes, and with a relatively uniform number of satellites per orbit (namely, 264, 240, 210, 210, 200, 190, and 180 satellites, respectively). Here, we complement the previous studies on constellation design, by looking at the performance metrics from the point of view of positioning, and in particular of the tradeoff between a good coverage (expressed as a good $C/N_0$ and good GDOP) and a low cost of building the system (expressed as the number of satellites, orbits, and orbital planes). The drag force is also taken into account in our study.

## III. THREE-SEGMENT ARCHITECTURE OF ANY PNT SATELLITE SYSTEM

Fig. 1 illustrates the three-segment architecture of any PNT satellite system. The space segment of the SIS segment refers to the sum of satellites in the sky belonging to a certain LEO-PNT system. The main SIS design parameters include parameters regarding the orbits (e.g., type, inclination, altitude, etc.), the number and sizes of the satellites on each orbit, and the satellite transmitter characteristics, typically optimized based on link-budget analysis and regulations. This article focuses on the orbital design features as well as on link-budget analysis. The ground segment refers to the Earth station or stations which are sending uplink (UL) signals to the satellites in order to monitor and control them. Design considerations related to the ground control center include, but are not limited to: the number and geographical placements of the ground control and monitoring center(s), the UL signal characteristics (carrier frequency, bandwidth, modulation, coding, etc.), the ground antenna design, etc. The user segment refers to the sum of user devices (or receivers) having the ability to compute the user's positions based on the signal received from the satellites. Design considerations in the user segment refer, for example, to the types of positioning methods (e.g., code-based, angle-based, Doppler-based, etc.), the demodulation and channel decoding stages, the choices of the signal bandwidth and sampling rates, as well as the possibility of joint positioning and communication tasks.

For sake of compactness and because the SIS design is already a broad topic, this article focuses only on SIS design challenges. Future work will also address the design considerations related to ground and user segments in LEO-PNT, as currently these parts are also insufficiently addressed in the current literature to the best of our knowledge.

## IV. CONSTELLATION DESIGN

The SIS design is first and foremost related to the constellation design. Such constellation design is one of the most critical and most difficult stages in the design of the space system of a new satellite constellation, as there are many degrees of freedom, such as the orbit type (i.e., polar, sun-synchronous, etc.), the constellation architecture/shape (i.e., Walker Delta, Ballard Rossette, Flower, etc.), the orbital heights, the orbit inclination, the number of orbits/orbital planes, the number of satellites in each orbital plane, and the other orbital parameters, such as the right ascension of the ascending node (RAAN), rate of perigee rotation, drift between satellites (e.g., for several orbital planes with different inclinations, satellites will drift apart), etc. We address below the main constellation design parameters which are directly related to SIS design. We also discuss the known advantages and disadvantages of each possible choice.

### A. Orbit Type

The possibilities for the satellite orbits are very diverse. A classification of the most used orbit types is listed below, according to their altitude, direction, inclination, eccentricity, and synchronicity.

*1) Altitude:*

*a) LEO:* Geocentric orbits with altitudes between 200 and 2000 km.

*b) MEO:* Geocentric orbits with altitudes ranging from 2000 to 35786 km.

*c) GEO:* Geosynchronous orbit that matches Earth's orbital period—taking 23 h 56 min and 4 s. This happens at an orbit altitude of exactly 35 786 km.

*d) High Earth orbit (HEO):* Geocentric orbits above 35 786 km.

*2) Direction:*

*a) Prograde-orbits or direct orbits [18]:* The satellite moves in the same direction as the Earth's rotation (e.g., GNSS MEO satellites and Amazon Kuiper LEO satellites).

*b) Retrograde-orbits [18], [19]:* The satellite moves in the opposite direction with respect to the Earth's rotation (e.g., OneWeb and Blacksky Global LEO satellites).

*3) Inclination:*

*a) Inclined orbits: a1) Polar Orbits [20]:* In a strict-sense definition, the orbital inclination angle is ± 90° (i.e., the satellites travels around the Earth from pole to pole). However, according to the European Space Agency (ESA), also angles close to 90° are referred to as polar (e.g., Iridium LEO satellites, with inclinations of 86.4° are considered as having polar orbits). *a2) Polar sun-synchronous orbit (SSO)* is nearly polar orbits (orbits with an inclination angle of ≈ 90°) that pass the equator at the same local solar time on every pass. It means

that a satellite is visible from a specific location at the same local time.

*b) Noninclined orbits: b1) Equatorial Orbits:* These orbits lie close to the Earth's equatorial plane. The orbital inclination is 0° for prograde orbits, and 180° for retrograde orbits. *b2) Ecliptic Orbits:* These orbits lie in the ecliptic plane, which is defined as the imaginary plane containing the Earth's orbit around the sun.

*c) Near equatorial orbits:* Similar to equatorial orbits, but their inclination is not strictly zero.

*4) Eccentricity:*

*a) Circular orbit:* It is an orbit that has an eccentricity equal to 0, and whose orbit traces a circle.

*b) Elliptic orbit:* It is an orbit that has an eccentricity greater than 0 and lower than 1, and whose orbit traces an ellipse.

*c) Parabolic orbit:* It is an orbit with an eccentricity equal to 1. These orbits have a velocity equal to the escape velocity (a velocity greater than the velocity to escape the gravitational pull of the planet).

*d) Hyperbolic orbit:* It is an orbit with eccentricity greater than 1.

*5) Synchronicity:*

*a) Synchronous orbits: a1) Sun-synchronous orbits* are particular types of polar orbits, where a satellite is always seen at a certain hour of the day at the same point of the Earth (e.g., a satellite is visible in Helsinki city exactly at noon each day), which means that the orbital planes are synchronized to always be in the same "fixed" position relative to the Sun. *a2) Sun-geosynchronous orbits* are similar to SSOs, but the satellites motion is synchronized with the Earth instead of the Sun. This type of orbit is typically implemented at high altitudes, beyond LEO and MEO.

*b) Subsynchronous orbits: b1) 12-h semi-synchronous orbits* are geosynchronous orbits, where the rotational period is half the Earth. *b2) Molniya orbits* [21] are highly elliptical orbits with an inclination of 63.4°, an argument of perigee of 270°, and an orbital period of approximately 12 h. This particular orbits give much better coverage at high altitudes (beyond LEO and even MEO).

According to the classification given above, MEO GNSS constellations use circular, semi-synchronous, prograde, and inclined orbits. Regarding LEO systems, the most common is to find LEO constellations using circular, polar, prograde, and semi-synchronous orbits. Although no LEO-PNT-specific constellation and orbit type can be found in the literature, by analogy with GNSS MEO constellations, we believe that a well-suited orbit type for LEO-PNT would be also a circular, prograde, and semi-synchronous orbit. Such a choice could offer to the constellation the symmetry needed for equal coverage, synchronicity in the visible satellites, and a lower launching cost than other more complex orbit types.

## B. Constellation Architecture

The constellation pattern influences the choice of the number of satellites needed to achieve certain performance targets (e.g., good coverage and as well as the link-budget considerations), addressed later on. Regarding the constellation pattern,

there are currently many constellation types/architectures in the literature. Some of the most typically studied are as follows.

*1) Walker Constellation [8], [22]:* There are two main types of Walker constellation: 1) Walker Star and 2) Walker Delta (also called Ballard Rosette). Walker constellations are by far the most encountered constellation types, based on symmetrical circular orbits (i.e., orbital planes) around the Earth, all having the same inclination and same eccentricity. In Walker Star [23] constellations, all the orbits cross near the Earth's Poles. The orbital planes are evenly spaced along the Earth, and half of them are counter-rotating (i.e., in half the orbital planes, the satellites movement is moving away from the north pole, and the other half is moving toward the north pole). Walker Delta [23] constellations are similar to Star ones, but more generalized than just considering the polar case and the total set of satellites are evenly distributed in each orbital plane. Galileo MEO constellation, for example, is based on Walker Delta orbits and provides a continuous Earth coverage of at least four satellites. Circular orbits have zero eccentricity parameters. Some LEO systems using Walker constellations are OneWeb [2] and Iridium [17]. The real eccentricity is not exactly zero, due to nonideal phenomenon in the trajectories (e.g., eccentricity is about $\epsilon = 0.00015$ for OneWeb and Iridium). Fig. 2(a) shows an example of an $N_{sv}/N_p/F = 24/6/2$ Walker Delta constellation.

*2) Elliptical-Orbit Constellation [24], [25]:* It also known sometimes under the name of a highly elliptical orbit (HEO)—is very similar to a Walker constellation, but each satellite orbit has now an elliptical shape instead of a circular one.

*3) Flower Constellation [8], [26], [27]:* It is a type of constellation whose orbit relative to the Earth-centered Earth-fixed (ECEF) coordinate framework resembles to flower petals. By choosing different orbits in a flower constellation, one can optimize each orbit to a particular latitude region (e.g., Equatorial, polar, etc.) in such a way that the sum of the orbits will cover the whole Earth according to certain target metrics. Fig. 2(b) shows an example of Flower constellation.

*4) Street-of-Coverage Constellation [23]:* It refers to multiple circular orbits, with the same orbital centers placed at exactly the same altitude. It is similar to a Walker constellation, but in which the orbital planes are unevenly spaced.

The current literature on LEO satellites points out toward Walker orbits as the orbits of choice in current systems. For an LEO-PNT system, it remains an open research topic how to optimize the constellation design. One solution is to adopt an optimization based on GDOP, as GDOP was previously shown [6] to be related to positioning performance. Other constellation-optimization works can be found, for example, in [7], [15], and [28]. An altitude optimization based on $C/N_0$, Cramer–Rao lower bound (CRLB) [29], [30], [31], GDOP, and drag factor is presented later in this article in Section VI.

## C. Coverage Considerations

The satellite coverage area is defined as the region of the Earth where a single satellite is seen at a certain minimum
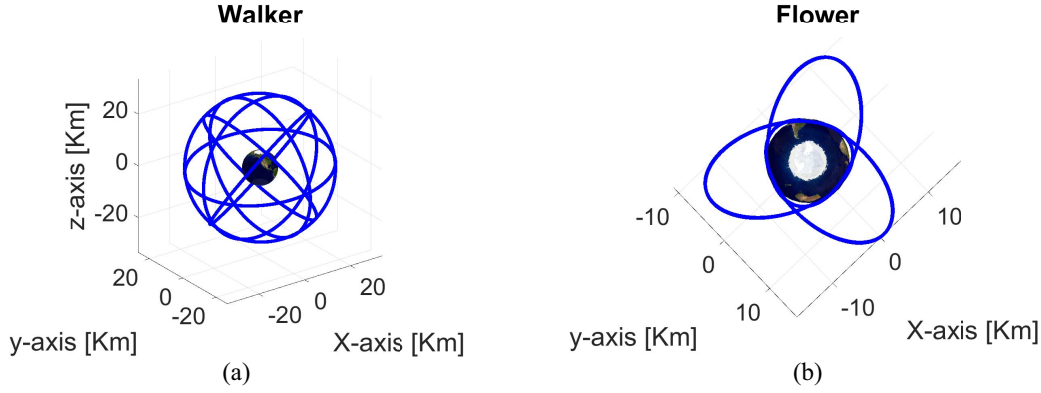
**Walker**

**Flower**



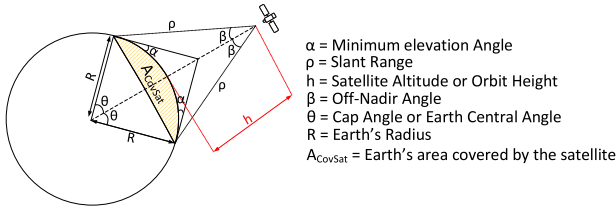Fig. 2.   Illustrative examples of two constellation shapes: (a) Walker and (b) Flower.



Fig. 3.   Illustrative example of coverage per satellite $2\theta$, cap angle $\theta$, elevation angle $\alpha$, and altitude $h$.

elevation angle defined by the system/application (e.g., typically 10° in GNSS). This coverage area depends on the satellite orbit of the specific constellation. One way to measure how good is the coverage of a certain satellite constellation largely used in the literature is by means of the dilution of precision (DOP), and more specifically, the geometric DOP or GDOP, a metric related to both the coverage and the positioning accuracy [6]. The smaller the GDOP value is, the better the accuracy of positioning solution is expected to be and the better the Earth coverage is [32]. Traditionally, a GDOP value of 1 was considered as "ideal," but with the advent of LEO constellations with very large number of satellites, values below 1 have also become realistic [6]. Fig. 3 illustrates a simplified approach of computing a coarse approximation of the coverage area on Earth with a certain satellite. The satellite is assumed to be placed at an altitude $h$ from the Earth's surface, and it has a minimum elevation angle (or elevation mask) $\alpha$ (below this elevation mask, the satellite is no longer "seen," as it will go below the horizon). The maximum Earth central angle, also called cap angle $\theta$, defines the Earth coverage via $2\theta$. The $\rho$ edge represents the slant range and $R$ denotes the Earth radius.

It follows from Fig. 3 and generalized Pythagoras formulas that:

$$(R + h)^2 = R^2 + \rho^2 - 2 \cdot \rho \cdot R \cdot \cos(90° + \alpha) \qquad (1)$$

where $\alpha$ above is given in degrees. Equation (1) has two solutions, but only the positive one (denoted by $\rho$) makes physical sense

$$\rho = -R\sin(\alpha) + \sqrt{R^2\sin^2(\alpha) + 2Rh + h^2} \qquad (2)$$

where $\rho$ is the slant range, $R$ is the Earth's radius, $\alpha$ is the elevation mask, and $h$ is the orbit altitude. We can compute the satellite service area angle $\beta$ as

$$\beta = \sin^{-1}\left(\frac{R}{(R + h)} \cdot \sin(\alpha)\right) \qquad (3)$$

and the cap angle $\theta$ as

$$\theta = \cos^{-1}\left(\frac{R}{(R + h)} \cdot \sin(\alpha)\right) - \alpha. \qquad (4)$$

### D. Orbital Altitude

The choice of satellite altitude and constellation in a satellite system has a significant impact on the performance and cost of the system. Altitude affects the received signal strength because it influences the attenuation due to atmospheric losses (e.g., the particles density which produces attenuation decreases at higher altitudes) as well as the Doppler effect (e.g., the lower the altitude is, the more affected the satellites are by the Earth gravity, and the higher the Doppler shift is). For more details about the orbit-altitude choice, one can refer to [1]. Section VI will also present our approach for LEO-PNT altitude optimization based on positioning-related metrics.

### E. Orbital Inclination

The optimal orbital inclination corresponds to the minimum inclination giving the maximum coverage area. Fig. 4 shows the minimum inclination needed for global coverage as a function of the altitude for three different elevation masks. According to [33], this minimum inclination angles can be computed as

$$i_{\min} = \max(\Phi_{\max} - \theta, 0) \qquad (5)$$

where the cap angle $\theta$ was given in (4) and $i_{\min}$ is the minimum inclination angle in degrees, and $\Phi_{\max}$ is defined as $\max(|\phi_l|, \phi_u)$, with $\phi_l$ and $\phi_u$ being the minimum and maximum latitudes within the coverage area, respectively. For full Earth coverage from −90° to +90° latitudes, $\Phi_{\max} = 90°$.

### F. Number of Orbits

The number of planes of a constellation determines how many independent trajectories the satellites take. In each of these planes, a certain number of satellites can be placed. The
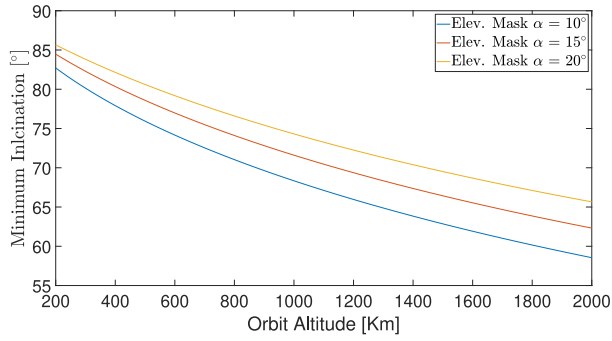
Fig. 4.   Example of the minimum inclination per orbit needed for full coverage (from $-90°$ to $+90°$ latitude) as a function of the orbit altitude for three different elevation masks.
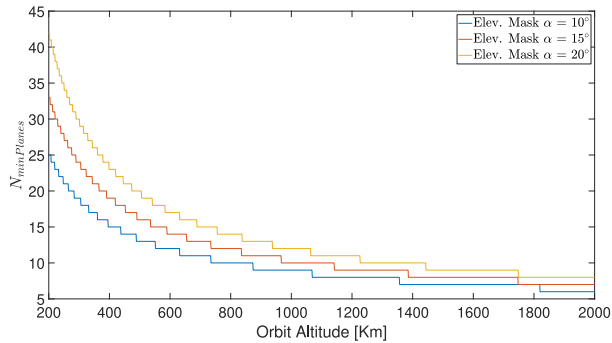


Fig. 5.   Example of the minimum number of orbital planes needed to cover the Earth as a function of orbit altitude for different elevation masks.
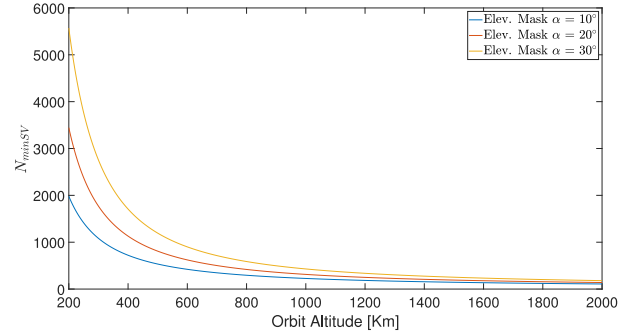


Fig. 6.   Example of the minimum number of satellites in the constellation needed for a full 4-fold coverage at different elevation-angle masks.
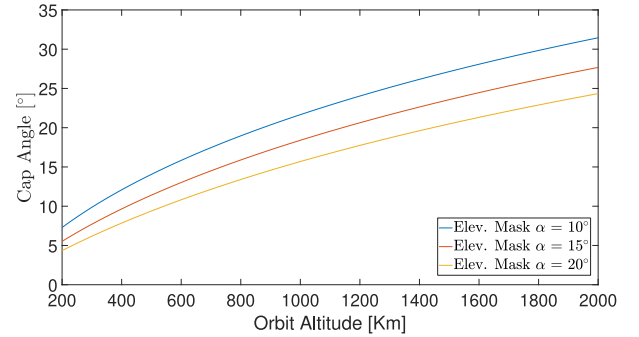


Fig. 7.   Example of average cap angle $\theta$ at various orbital heights and satellite elevation mask for a Walker constellation.

number of planes is selected in relation to the wanted coverage, under the constraint of a maximum allowed complexity of the constellation. A higher number of orbits will typically give better coverage, but both the complexity and cost will be increased as well, since more independent launches will be needed and more satellites will need to be put into orbit. The number of orbits needed to cover the whole Earth is inversely proportional to the altitude, since as higher the orbit altitude is, bigger becomes the coverage angle $\theta$, and less satellites are needed to cover the whole Earth. The minimum number of orbits to give global coverage can be computed as

$$N_{\mathrm{minPlanes}} = \frac{360}{2\theta} \qquad (6)$$

where $\theta$ is the cap angle in degrees shown in Fig. 3.

   Fig. 5 shows the minimum number of orbits needed for giving global coverage as a function of the orbit altitude for different elevation masks.

### G.  Minimum Number of Satellites in the Constellation

   Another important aspect to consider is the number of satellites in the constellation. As more satellites are fit into the sky, more satellites will be in view at a specific time instant and location. But if this number is excessively large, the geometry offered by the constellation will not be optimal, giving similar satellite-in-view geometry and poor GDOP due to satellite redundancy. In addition, the launching cost and maintenance of the constellation will become excessively large. Therefore,

the number of satellites to be put in orbit has to be minimized, having in mind the service we want to provide (i.e., global/regional coverage, 1-fold/4-fold, etc.) and the cost we can handle. Hence, we can compute the minimum number of satellites in the constellation as [34]

$$N_{\mathrm{minSV}} = \frac{4K}{(1 - \cos(\theta))} \qquad (7)$$

where $K$ is the desired $K$-fold coverage (i.e., $K = 1$ for 1 satellite in view in any Earth's location and time instant, $K = 4$ for 4 satellites in view, etc.).

   In Fig. 6, we depict the minimum number of satellites needed for a 4-fold coverage, given different LEO orbit altitudes and elevation masks. As we can observe in Fig. 6, for low altitudes (e.g., 200–600 km), the required number of satellites decreases exponentially. Then, it becomes more linear. At this very low altitudes, we need more than 1000 satellites, while at higher altitudes, we will only need a few hundred. The different elevation mask angles differentiate more at low than at high altitudes, given the fact that at higher elevations the coverage per satellite is much bigger, as it is shown in Fig. 7.

### H.  Summary of Tradeoff in Constellation Design Parameters

   Table II summarizes the design tradeoff parameters while defining an LEO-PNT satellite constellation. One needs to choose parameters, such as the constellation type, orbit altitude, the number of orbital planes, the number of satellites per orbital plane, eccentricity, etc., based on target metrics, such as the desired coverage, the constellation complexity, the

| SIS design parameter | Design criteria for the considered design parameter in constellation design and observations |
|---|---|
| Constellation type | Trade-off: coverage, geometry, accuracy ( e.g., GDOP, $C/N_0$, CRLB) versus complexity and cost. Constellation type can be chosen, for example, via code GDOP-based optimization [6] or area percent coverage [14]. |
| Number of orbital planes | Trade-off: complexity (cost) of launch versus coverage and geometry/GDOP |
| Number of satellites per orbital plane | Can be optimized in such a way to have at least $N$ satellites in view (e.g., $N > 3$) at any point of Earth for good PNT performance; it depends on the orbit height and on the elevation angle above which a satellite is considered 'good' for positioning. |
| Orbit altitude (or semi-major axis of the orbit) | Trade-off: higher altitudes mean lower orbital speed, lower Doppler shifts, longer on-orbit times, and better coverage with a fixed number of satellites per orbit. However, launching and de-orbiting a satellite at higher orbits is typically more costly than at a lower orbit, and path-losses are higher from satellites at higher orbits when compared at the same carrier frequency with satellites in lower orbits. |
| Orbit Eccentricity (or 'flatness' of the ellipse) | Can be optimized for best geometry (e.g., code/Doppler GDOP-based optimization). Typically, the circular orbits (zero eccentricity) are the most encountered in current LEO satellite systems. |
| Signal carrier frequency | Trade-off: bandwidth, antenna size, path loss, spectrum regulations. Smaller carrier frequencies mean larger antennas and smaller available bandwidths; larger carrier frequencies mean larger path losses and higher sensitivity to rain, mist, clouds, and various gases in the atmosphere. Most mega-constellations nowadays use Ku and Ka bands, namely carrier frequencies between 13 GHz and 40 GHz (Iridium Next, Amazon Kuiper, Space X Starlink,...). |

cost to lunch/maintain the constellation, and the positioning accuracy-related metrics (e.g., CRLB, $C/N_0$, GDOP, etc.). The higher the altitude is, the lower the Doppler shifts are and the bigger the coverage area per satellite is. At the same time, the higher the altitude is, the higher the path losses are and the more costly the launching/de-orbiting of the satellites is. The optimal carrier-frequency choice is determined by aspects, such as the available application bandwidth, receiver and transmitter antenna sizes, the maximum path losses that the system can handle, the spectrum regulations, etc.

## V. LINK-BUDGET-RELATED AND GEOMETRY-RELATED CONSIDERATIONS

In this section, we first revise a basic link-budget model and we then model the received $C/N_0$ based on this model in concrete examples based on eight selected constellations. We then focus also on examples related to the geometry of the constellations, by showing the average number of visible satellites and average GDOP for the same eight constellations.

The link budget consists of an analysis of the received signal strengths at the transmitter side, in both UL and downlink connections, by taking into account path-loss models in order to estimate the losses over the wireless channel as well as the achievable CNRs for a specific system. In the LEO-PNT context, the downlink propagation (from the satellite to the Earth receiver) is the one of interest in terms of positioning targets and therefore the analysis here will focus on downlink transmission. Widely speaking, the received signal strength $P_R$ depends on the transmitted signal strength $P_T$ via

$$P_R = P_T + G - PL \qquad (8)$$

where $G$ is the sum of all gains in the transmission chain (e.g., transmitter and receiver antenna gains) and PL is the cumulative path loss over the wireless channel, which depends on the transmitter–receiver distance, on the carrier frequency $f_c$, on the various atmospheric effects (e.g., gaseous and rain absorption, and tropospheric and possibly ionospheric absorption), and on the terrestrial scenario (e.g., absorption due to reflections, scattering, and refraction on buildings and trees, wall losses for indoor propagation, etc.). A simplified path-loss model adopted, for example, in QuaDRiGa [35], [36] framework for a realistic satellite-to-ground channel modeling is as follows:

$$\mathrm{PL[dB]} = A\log_{10}(d(h)/d_0) + B + C \cdot \log_{10}(f_c/f0) + \eta \quad (9)$$

where $d(h)$ is the 3-D distance between the satellite and the Earth receiver, and therefore it is dependent on the satellite altitude $h$, $d_0$ is a reference distance, typically taken as $d_0 = 1$ m, $f_c$ is the carrier frequency, $f0$ is a reference frequency (here 1 GHz) and $A$, $B$, and $C$ are scenario-specific coefficients, typically obtained by measurements. $A$ [in dB/$\log_{10}(m)$] corresponds to the 3-D distance path loss (e.g., in free-space path loss $A = 20$), $B$ (in dB) corresponds to the reference path loss at 1 GHz and 57.3° elevation (e.g., in free-space path loss $B = 32.45$), and $C$ [in dB/$\log_{10}$(GHz)] corresponds to the frequency-dependent path loss (e.g., in free-space path loss $C = 20$). Full details on the parameters choice can be found in [35] and [36]. These coefficients include atmospheric effects, multipath propagation effects, receiver and transmitter antenna effects, etc. In addition to the deterministic effects modeled in the first part of (8) and (9), random effects due to shadowing and fading are also occurring [35], [36], [37] and they are lumped here under the noise variable $\eta$,
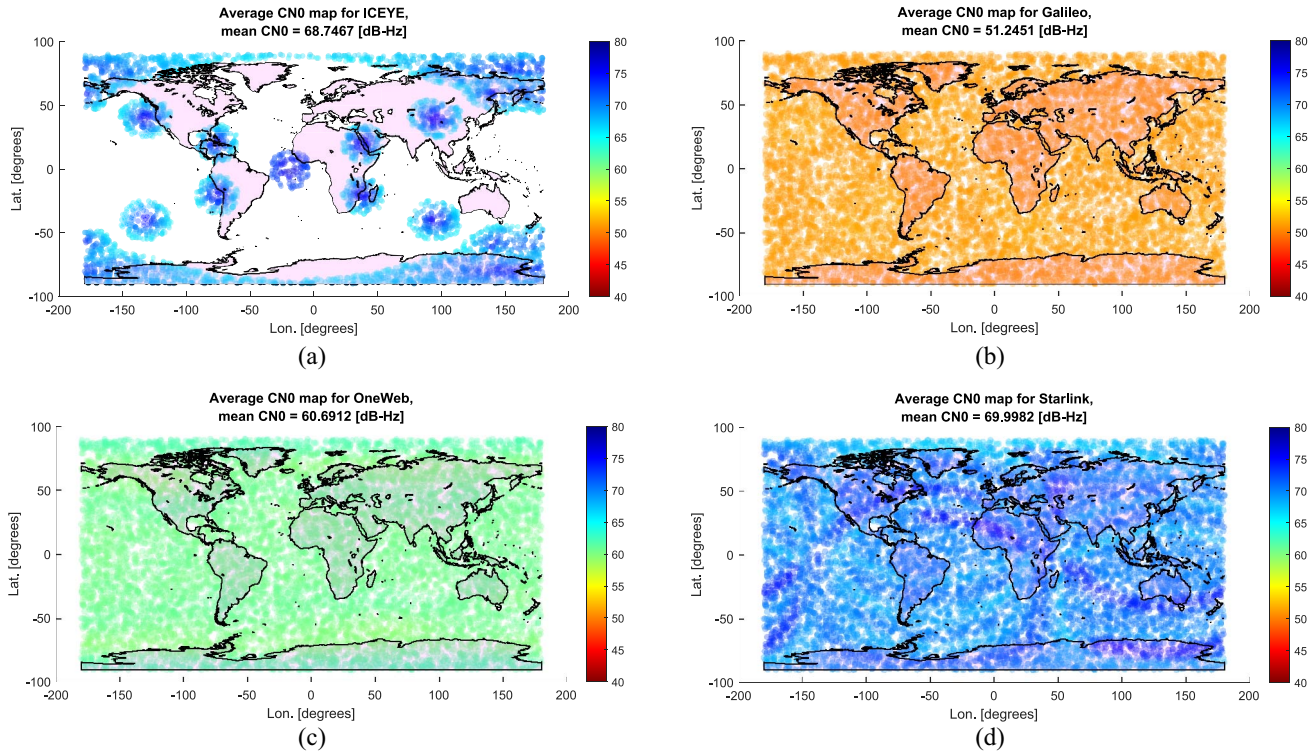
Fig. 8.    Average $C/N_0$ for eight different constellations: (a) ICEYE (LEO, small); (b) Galileo (MEO); (c) Oneweb (LEO, mega); and (d) Starlink (LEO, mega).

assumed to be Gaussian distributed of zero mean and a certain shadowing/channel variance $\sigma_{ch}$.

During our simulation-based analysis, we have generated a wireless channel propagation based on QuaDRiGa models and assuming a satellite transmit power between 45 and 65 dBm, according to each considered LEO constellation (based on values found in [38], [39], [40], [41], and [42]). Also, according to [37], we considered multipath propagation with 6–10 channel paths and we have adopted a line-of-sight (LOS) outdoor propagation in order to compare MEO and LEO $C/N_0$. We have selected eight existing constellations for comparative purposes, with six LEO and two MEO ones. The six LEO constellations comprise three large constellations (OneWeb, Amazon Kuiper, and SpaceX Starlink) and three small constellations (Astrocat, Myriota, and ICEYE). The two MEO constellations are based on Galileo and GPS.

Fig. 8 shows the mean received $C/N_0$ across the Earth for four different LEO and MEO constellations picked as examples in an outdoor LOS scenario. The $C/N_0$ was measured as the average $C/N_0$ of signals received from the satellites in view for each specific user position at a certain time instant. For considering in-view condition, we just took into account the satellite elevation from the user position, which needed to be above 10°. Fig. 8 shows that the received $C/N_0$ for LEO constellations can be up to about 10–15 dB–Hz higher than for MEO (for clarity we only show here the MEO Galileo, but similar observations were done for other MEO GNSS). Fig. 9 shows the number of satellites in view along the Earth for different receivers. We can see that for small-sized

LEO constellations (here ICEYE is shown as an example, but similar results were observed for Astrocast and Myriota) the mean number of satellites in view is very low (between 1 and 3), and some areas are not covered at all (white holes in Fig. 9). This makes this current constellations nonusable for positioning ($\leq 4$ satellites in view), but an update with additional satellites/orbital planes might increase the coverage and its feasibility for LEO-PNT. At the same time, megaconstellations (here OneWeb and Starlink are shown, but similar observations were noticed from Kuiper) can have hundreds of satellites in view at each Earth point, due to their huge amount of satellites in the sky. For setting up these three constellations, we have considered the potential final constellation [40], [41], [42]. For example, Starlink will have 34 408 [40] satellites in the final, yet-to-be fully launched constellation and an average of almost 500 satellites in view, Kuiper will have 7774 [42] satellites in the sky and an average of 139 satellites in view on any Earth location, while Oneweb will be the largest one having 47 844 [41] satellites in view and an average of more than 2000 satellites in view. MEO constellations, namely, Galileo and GPS, have much lower constellations, namely, 27 (with around 8 in view in average) and 31 (with around 9 in view in average), respectively. These satellite-in-view numbers are obtained in ideal LOS conditions, considering 10° elevation mask and satellite beamwidth equal to the area of coverage. Most of the constellations analyzed in Fig. 8 fulfill the minimum required amount of satellites in view for positioning purposes and they show that there is a significant place for optimization of new LEO-PNT constellations with a significant lower number of satellites in orbit.
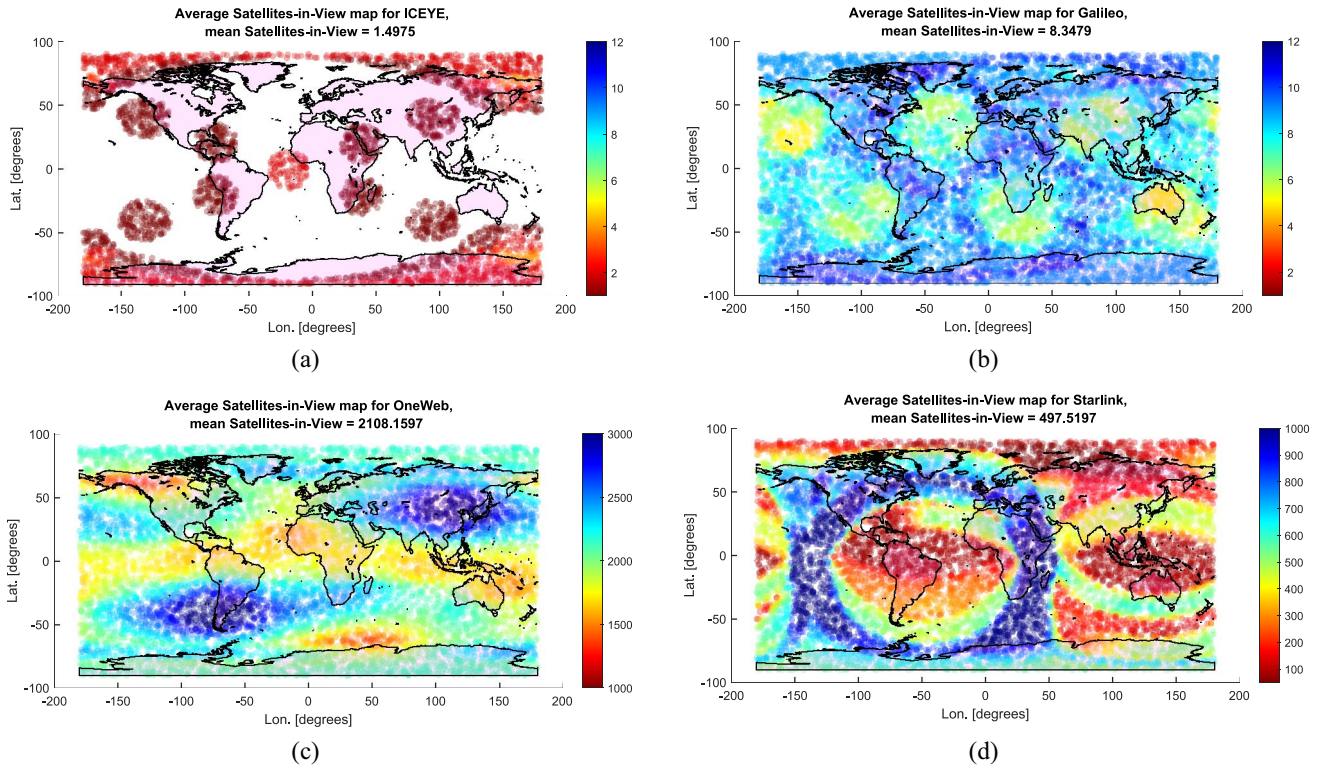
Fig. 9. Example of the number of satellites in view for eight different constellations: (a) ICEYE; (b) Galileo; (c) Oneweb; and (d) Starlink.

TABLE III
COMPARISON BETWEEN MEO AND LEO CONSTELLATIONS IN TERMS
OF GDOP, AVERAGE $C/N_0$, AND AVERAGE NUMBER OF
SATELLITES-IN-VIEW PER EARTH POINT
(LOS OUTDOOR SCENARIO)

| Constellation | GDOP | Average $C/N_0$ [dBHz] | Average # of satellites in view |
|---|---|---|---|
| MEO, Galileo | 4.56 | 56.8 | 8.55 |
| MEO, GPS | 5.4 | 49.5 | 9.5 |
| MEO, GLONASS | 4.5 | 48.5 | 7.7 |
| MEO, BeiDou | 4.6 | 57.8 | 7.3 |
| LEO, Starlink | 4.6 | 102.1 | 8297.6 |
| LEO, OneWeb | 0.8 | 72.1 | 1690.1 |
| LEO, Kuiper | 7.5 | 78.5 | 712.12 |
| LEO, Astrocast | 13.1 | 48.2 | 20.2 |
| LEO, Hiber | 2.4 | 59.5 | 6.4 |
| LEO, ICEYE | 4.5 | 34.0 | 4.5 |

Table III summarizes the $C/N_0$ and mean number of satellites in view for six LEO and all four MEO GNSS constellations (GPS, Galileo, Beidou, and Glonass). Additionally, it also shows the average GDOP values. A lower GDOP value means that the constellation offers a better geometry than a higher GDOP-values constellation, and a low GDOP avoids precision inaccuracies due to nonoptimal satellite positions and is therefore highly suitable for positioning purposes.

Figs. 8 and 9 as well as Table III show that typically average $C/N_0$ and the average number of satellites in view are interrelated (a higher $C/N_0$ can typically be achieved with a larger constellations), but that a good GDOP is not necessarily achieved with an increased number of satellites in the sky. For example, OneWeb constellation has the best average GDOP but it has a lower amount of satellites in the sky than Starlink; also MEO constellations have good GDOP values, comparable to megaconstellations such as Starlink, despite their low number of satellites in the sky. This analysis also shows that a good SIS design for an LEO-PNT system does not necessarily need to rely on a large number of satellites and there is a place for optimization methods, to be investigated in further studies, to achieve simultaneously good GDOP, a minimum of 4 satellites in view in every Earth point, and good $C/N_0$ level with a reduced number of satellites in the final constellation.

## VI. LEO OPTIMIZATION OUTCOMES AND DESIGN RECOMMENDATIONS

In this section, we make a feasibility analysis regarding LEO SIS design, based on realistic channel modeling via QuaDRiGa models described in the previous section. We address the question of how many satellites in the orbit will offer a good tradeoff between cost and coverage, what orbital altitudes are to be preferred, and what are some good choices of a carrier frequency for maintaining reasonable CNRs at the receiver. At the end of this section, we give some design recommendations for the LEO system based on our feasibility study. Regarding the constellation design, we have carried out an optimization procedure based on the findings in Sections IV-D–IV-G. We
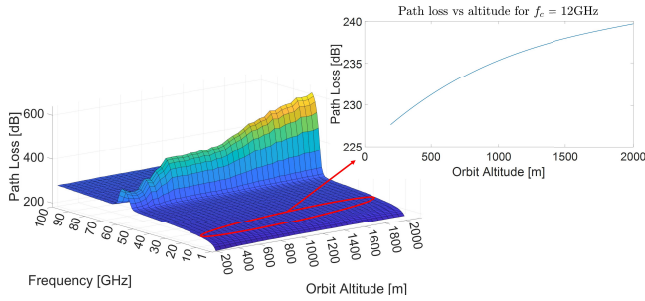
Fig. 10.   Example of path loss at different frequencies and orbit altitudes.



Fig. 11.   Normalized drag force experienced by a satellite as a function of the orbit altitude.

used the four normalized optimization cost functions given in (10)–(14)

$$\text{Cost1} = \frac{N_{\min}}{\max(N_{\min})} \tag{10}$$

where $N_{\min}$ is a vector containing the minimum number of satellites needed to cover the entire Earth at different LEO orbit altitudes, such as shown in Fig. 6. $\max(N_{\min})$ corresponds to the largest number of satellites needed to cover the Earth over all considered orbit altitudes (typically, this maximum occurs at 200-km altitude, the lowest LEO altitude)

$$\text{Cost2} = \frac{C/N_0}{\max(C/N_0)} \tag{11}$$

where $C/N_0$ is a vector containing all the $C/N_0$ measured at the receiver after the transmission through the wireless channel. $\max(C/N_0)$ represents the maximum received $C/N_0$ over all the considered altitudes. Fig. 10 gives an example of a Quadriga-based path-loss model [see (9)] considering different combinations of carrier frequencies and orbit altitudes. Fig. 10 shows that the higher the orbit altitude is, the higher the path losses are, as expected. With respect to the carrier-frequency choice, we observe a region from about 55 GHz to about 70 GHz where the losses are considerably higher compared to the rest of the frequencies and for all altitudes. This peak is due to high oxygen absorption around those frequencies.

The third cost function corresponds to the tracking variance error measurement and can be computed as

$$\text{Cost3} = \frac{\text{CRLB}_{\text{trackvar}}}{\max(\text{CRLB}_{\text{trackvar}})} \tag{12}$$

where $\text{CRLB}_{\text{trackvar}}$ is a vector containing the CRLB [31], [43] measurements of the positioning error variance, when distance estimates are based on time-of-arrival estimates for all considered orbit altitudes. $\text{CRLB}_{\text{trackvar}}$ depends on the available receiver bandwidth and on its $C/N_0$ and it is a measure of how good accuracy one can achieve in positioning. The value $\max(\text{CRLB}_{\text{trackvar}})$ corresponds to the highest $\text{CRLB}_{\text{trackvar}}$ over all the considered orbit altitudes. For more details about $\text{CRLB}_{\text{trackvar}}$, please check [29], [30], and [31].

Finally, the last cost function takes into account the orbit atmospheric effects. In particular, it takes into account the drag force experienced by the satellites as a function of the orbit altitude. A high drag force means less stable orbital parameters, and therefore, a target optimization criterion is to avoid
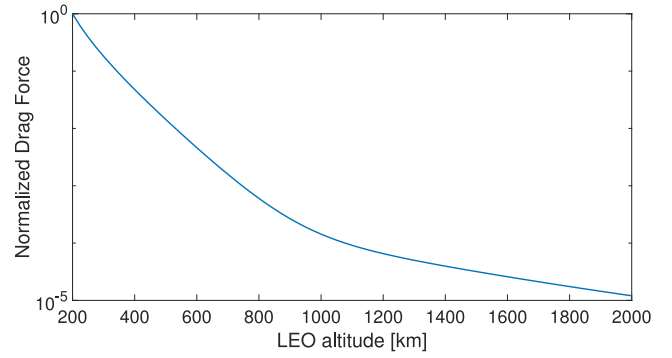
regions with high drag forces. $F_{\text{drag}}$ can be computed as

$$\text{F}_{\text{drag}} = \frac{1}{2} \cdot \rho \cdot V^2 \cdot C_d \cdot A_{\text{CovSat}} \tag{13}$$

where $A_{\text{CovSat}}$ is the reference surface area, which can be computed as $2\pi R_e^2 (1 - \cos\theta)$, where $\theta$ is defined in (4). $Cd$ is the drag coefficient, considered as constant and equal to 2.2 [44]. $V$ is the relative velocity of the satellites with respect to the atmosphere (in our simulations, we have considered a simplified model in which the atmosphere speed is in fact the Earth's rotation speed) and $\rho$ is the atmospheric density (in our simulations computed as an annual average atmospheric density using the MSIS-86 model [45]). Fig. 11 shows the drag force experience by a satellite as a function of the altitude. We can observe that from about 600 km the drag force is not that noticeable, being $< 1e^{-3}$. The cost function considering the drag force can be computed as

$$\text{Cost4} = \frac{F_{\text{drag}}}{\max\left(F_{\text{drag}}\right)} \tag{14}$$

where $F_{\text{drag}}$ is the drag force experienced by the satellites and $\max(F_{\text{drag}})$ is the maximum drag force experience at any orbit altitude (which corresponds to the lowest orbit altitude).

The overall cost function for optimization is defined as the sum of all normalized cost functions described in (10)–(14), taking into account if they need to be minimized (Cost1, Cost3, and Cost4) or maximized (Cost2)

$$\text{Cost}_T = \text{Cost1} + \frac{1}{\text{Cost2}} + \text{Cost3} + \text{Cost4}. \tag{15}$$

Cost1 depends on the orbit altitude. As higher the orbit altitude is, $N_{\min}$ becomes smaller. Cost2 also depends on orbit altitude, but it is inversely proportional (as higher the orbit altitude, the lower the $C/N_0$). Cost3 is directly dependant on $C/N_0$, that in turn it also depends on orbit altitude. Finally, Cost4 is higher at lower orbit altitudes.

Fig. 12 shows three different curves, based on three different carrier frequencies in the optimization cost functions by using (15) and considering a minimum elevation mask of 10°. Each curve corresponds to a different carrier frequency used in the transmitter, namely, 1, 3, 10, and 30 GHz. A transmitter power of 32 W, transmitter and receiver gain of 24 dB, and a receiver bandwidth of 5 MHz were used in the simulations.

TABLE IV
Design Recommendations Based on Our Feasibility and Optimization Studies for a Minimum Elevation Mask of 10°

| Design parameter | Design recommendations for LEO-PNT | Reason |
|---|---|---|
| Constellation type | Walker Delta | Analogy with GNSS; Best average GDOP due to better geometry; Easiness of launching; Satellites from adjacent orbital planes move in opposite directions, giving distinct Doppler frequencies |
| Orbit Altitude | $500 - 1050$ km | The lower altitude, the lower the path losses are (see Fig. 10). However, the lower the altitude, the more the satellites are influenced by the drag effect caused by the Earth attraction (see Fig. 11) and more satellites are needed to cover the Earth since the coverage per satellite is lower. Reversely, the higher altitudes better coverage per satellite is provided but the signal is more attenuated. The optimal range with a 10% error margin was found between 300 and 1025 km (see Fig. 12); due to the drag force, we recommend the altitude design range between 500 and 1050, with an optimum at 600 km based on our current optimization metrics. |
| Number of orbital planes | $\geq 14$ | According to 6 we need at least 6 orbital planes at LEO altitudes. There is a trade-off performance-cost, as it is more costly to launch satellites in different orbital planes than in the same orbital planes (we need individual launching for each orbital plane). For 600 km altitude, we need at least 14 orbital planes as shown in Fig. 6 |
| Number of satellites | $\geq 450$ | According to Fig. 7 we need approximately 450 satellites at the 600 km altitude for providing a 4-fold Earth coverage |
| Orbit Eccentricity (or 'flatness' of the ellipse) | As close to 0 as possible | $\epsilon = 0$ is the most encountered eccentricity in the current LEO systems due to good symmetry and constant satellite velocity |
| Inclination | $\geq 75°$ | Based on our optimization study we need at least 75° for providing global coverage considering a minimum satellite elevation mask of 10° (see Fig. 5) |
| Carrier Frequency | Preferably below 10 GHz and necessary to avoid 55-75 GHz band in which oxygen absorption loss is very high | See Fig. 10. Lower carrier frequencies are better from the link budget point of view (better indoor penetration) |

Regarding the channel, an outdoor LoS scenario was considered. As we can see in Fig. 12, for all four frequency bands, the results are pretty similar and point out toward the same optimal orbit altitudes, independently of the carrier frequency. The optimal altitude given by the optimization in (15) is approximately 600 km. We have included a 1% margin in order to consider nonidealities, such as additional de-orbiting time, Doppler effects, etc. With this margin, the optimal altitude range is extended from about 500 to 700 km. Comparing Fig. 12 with Fig. 11, this is exactly where the drag force starts to be not as strong as at lower orbits. In addition, the $C/N_0$ is higher than at higher orbits (with lower $F_{\text{drag}}$) and the number of satellites needed for a 4-fold coverage (Fig. 6) starts to become flat. Moreover, once the optimal altitude is evaluated, one can further determine that the minimum number of satellites to cover the whole Earth from Fig. 6. Our analysis based on the optimization described above gives a minimum of about 212 satellites distributed in 12 orbital planes, as observed in Fig. 5. One can further evaluate that the optimal orbital inclination of such a system would be about 75°–85° by simply looking at Fig. 4.

In addition, based on the examples from Fig. 10, we can say that the range 55–70 GHz should be avoided while selecting the carrier frequency for the LEO-PNT systems.

Table IV summarizes the constellation design recommendations based on our study. We propose to use a Walker Delta constellation architecture due to its good coverage, good geometry capability, and relatively low launching cost. Based
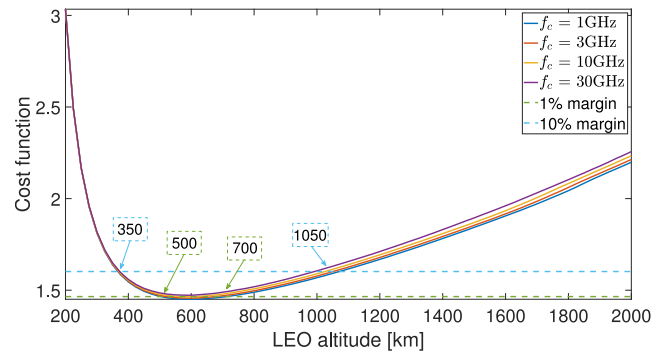


Fig. 12. Illustrative example of optimization output using the four cost functions and four different frequency bands: 3, 5, and 30 GHz. 1% and 10% error margins are also shown.

on our study, the constellation will need at least six independent orbital planes to cover the whole Earth at LEO orbit altitudes. The constellation will need between 55 and 1000 (depending on the minimum elevation mask threshold) satellites for providing a 4-fold coverage. The orbit eccentricity is recommended to be 0, or as close as possible to 0, by analogy with MEO GNSS orbits. Moreover, by having a small eccentricity, the system will keep a good symmetry and constant satellite velocity. Finally, regarding the carrier frequency we propose to avoid the frequency range between 55 and 75 GHz, in order to avoid the large path-loss attenuation due to the oxygen absorption. Therefore, we suggest that lower carrier frequencies in the order of few GHz to few tens of GHz are

better suited than higher carrier frequencies as they ensure lower path losses and hence higher received power.

## VII. CONCLUSION AND OPEN RESEARCH DIRECTIONS

In this article, we have made a feasibility study for the SIS design of future LEO-PNT systems. We have shown that LEO constellations are good candidates to complement the current GNSS constellations due to their closer proximity to Earth, which potentially improve the $C/N_0$ levels compared to GNSS, which might be  very useful in urban and indoor scenarios. To sum up, LEO's main advantages with respect to current MEO constellations are a better overall link budget, higher received $C/N_0$ values due to their proximity to the Earth surface, relatively lower production and launching costs than for MEO ones, especially by using small-sized satellites, such as CubeSats, as well as higher satellite availability, meaning a larger number of satellites in view. In addition, LEO constellations have the potential of providing better in-sky geometries than MEO ones, which helps in achieving more accurate positioning, if designed properly. In this article, we have also given several recommendations regarding the constellation design of a hypothetical LEO-PNT constellation to be launched in the future, based on a simple optimization approach using $C/N_0$, CRLB, drag force, and GDOP as multiobjective optimization metrics. The chosen optimization criteria were selected to cover important aspects for positioning, such as the reception level ($C/N_0$), good geometry for positioning (here measured by GDOP), low drag force, and good accuracy of the positioning solution (here measured by CRLB). The optimization metrics can be further adjusted in accordance with the design needs, and a remaining open research question is how to reach the most suitable optimization criteria and optimization approaches in order to serve both code-based and Doppler-based positioning with future LEO-PNT solutions and to allow an easy integration of LEO-PNT and MEO GNSS solutions. Another open research point is regarding the detailed physical-layer design of the signal from the satellites, including signal modulation, optimal transmission bandwidth, pulse shaping type, channel coding scheme, multiple access scheme, etc.

## REFERENCES

[1] S. H. Mortazavi, "Orbit selection trade-offs for LEO observation microsatellites," in *Proc. AIAA SPACE Conf. Expo.*, Aug. 2015, pp. 1–11.

[2] T. Reid, A. Neish, T. Walter, and P. Enge, "Leveraging commercial broadband LEO constellations for navigation," in *Proc. 29th Int. Tech. Meeting Satellite Division Inst. Navig. (ION GNSS+)*, Sep. 2016, pp. 1–15.

[3] Y. Qian, L. Ma, and X. Liang, "Symmetry chirp spread spectrum modulation used in LEO satellite Internet of Things," *IEEE Commun. Lett.*, vol. 22, no. 11, pp. 2230–2233, Nov. 2018.

[4] C. Q. Dai, M. Zhang, C. Li, J. Zhao, and Q. Chen, "QoE-aware intelligent satellite constellation design in satellite Internet of Things," *IEEE Internet Things J.*, vol. 8, no. 6, pp. 4855–4867, Mar. 2021.

[5] A. Golkar and A. Salado, "Definition of new space—Expert survey results and key technology trends," *IEEE J. Miniat. Air Space Syst.*, vol. 2, no. 1, pp. 2–9, Mar. 2021.

[6] R. Morales-Ferre, E. S. Lohan, G. Falco, and E. Falletti, "GDOP-based analysis of suitability of LEO constellations for future satellite-based positioning," in *Proc. IEEE Int. Conf. Wireless Space Extreme Environ. (WiSEE)*, 2020, pp. 147–152.

[7] H. Ge, B. Li, L. Nie, M. Ge, and H. Schuh, "LEO constellation optimization for LEO enhanced global navigation satellite system (LeGNSS)," *Adv. Space Res.*, vol. 66, no. 3, pp. 520–532, 2020.

[8] G. Curzi, D. Modenini, and P. Tortora, "Large constellations of small satellites: A survey of near future challenges and missions," *Aerospace*, vol. 7, no. 9, p. 133, 2020.

[9] S. Abulgasem, F. Tubbal, R. Raad, P. I. Theoharis, S. Lu, and S. Iranmanesh, "Antenna designs for CubeSats: A review," *IEEE Access*, vol. 9, pp. 45289–45324, 2021.

[10] P. I. Theoharis, R. Raad, F. Tubbal, M. U. A. Khan, and S. Liu, "Software-defined radios for CubeSat applications: A brief review and methodology," *IEEE J. Miniat. Air Space Syst.*, vol. 2, no. 1, pp. 10–16, Jun. 2021.

[11] A. Nardin, F. Dovis, and J. A. Fraire, "Empowering the tracking performance of LEO PNT by means of meta-signals," in *Proc. IEEE Int. Conf. Wireless Space Extreme Environ.*, 2020, pp. 153–158.

[12] P. A. Iannucci and T. E. Humphreys, "Economical fused LEO GNSS," in *Proc. IEEE/ION Position Location Navig. Symp.*, 2020, pp. 426–443.

[13] N. Saeed, A. Elzanaty, H. Almorad, H. Dahrouj, T. Y. Al-Naffouri, and M. S. Alouini, "CubeSat communications: Recent advances and future challenges," *IEEE Commun. Surveys Tuts.*, vol. 22, no. 3, pp. 1839–1862, 3rd Quart., 2020.

[14] T. Savitri, Y. Kim, S. Jo, and H. Bang, "Satellite constellation orbit design optimization with combined genetic algorithm and semianalytical approach," *Int. J. Aerosp. Eng.*, vol. 2017, May 2017, Art. no. 1235692.

[15] P. Zong and S. Kohani, "Optimal satellite LEO constellation design based on global coverage in one revisit time," *Int. J. Aerosp. Eng.*, vol. 2019, pp. 1–12, Dec. 2019.

[16] H. Ge, B. Li, L. Nie, M. Ge, and H. Schuh, "LEO constellation optimization for LEO enhanced global navigation satellite system (LeGNSS)," *Adv. Space Res.*, vol. 66, no. 3, pp. 520–532, 2020.

[17] M. Guan, T. Xu, F. Gao, W. Nie, and H. Yang, "Optimal walker constellation design of LEO-based global navigation and augmentation system," *Remote Sens.*, vol. 12, no. 11, p. 1845, 2020.

[18] S. Cakaj, "Practical horizon plane and communication duration for low Earth orbiting (LEO) satellite ground stations," *WSEAS Trans. Commun.*, vol. 8, no. 4, pp. 373–383, Jan. 2009.

[19] J. Winn *et al.*, "HAT-P-7: A retrograde or polar orbit, and a third body," *Astrophys. J. Lett.*, vol. 703, p. L99, Sep. 2009.

[20] S. D. Ilcev, "Polar Earth orbits (PEO)," in *Proc. 20th Int. Crimean Conf. Microw. Telecommun. Technol.*, 2010, pp. 413–415.

[21] L. Riishojgaard, "High-latitude winds from molniya orbit—A mission concept for NASA's Earth system science pathfinder program," in *Proc. Int. Workshop Anal. Multitemporal Remote Sens. Images*, 2005, pp. 120–124.

[22] J. Davis, D. Mortari, and J. V. McAdams, "Reducing walker, flower, and streets-of-coverage constellations to a single constellation design framework *AAS*12 − 147, 22nd, spaceflight mechanics 2012," in *Proc. Adv. Astron. Sci. Spaceflight Mech.*, vol. 143, 2012, pp. 697–712.

[23] Y. F. Hu, G. Maral, and E. Ferro, *Appendix A: Satellite Constellation Design for Network Interconnection Using Non-Geo Satellites*. Hoboken, NJ, USA: Wiley, 2001, pp. 215–237.

[24] J. E. Velazco and J. S. de la Vega, "Q4—A CubeSat mission to demonstrate omnidirectional optical communications," in *Proc. IEEE Aerosp. Conf.*, 2020, pp. 1–6.

[25] R. L. Sturdivant and E. K. P. Chong, "Systems engineering of a Terabit elliptic orbit satellite and phased array ground station for IoT connectivity and consumer internet access," *IEEE Access*, vol. 4, pp. 9941–9957, 2016.

[26] D. Mortari and M. P. Wilkins, "Flower constellation set theory. Part I: Compatibility and phasing," *IEEE Trans. Aerosp. Electron. Syst.*, vol. 44, no. 3, pp. 953–962, Jul. 2008.

[27] M. P. Wilkins and D. Mortari, "Flower constellation set theory. Part II: Secondary paths and equivalency," *IEEE Trans. Aerosp. Electron. Syst.*, vol. 44, no. 3, pp. 964–976, Jul. 2008.

[28] Y. Han *et al.*, "LEO navigation augmentation constellation design with the multi-objective optimization approaches," *Chin. J. Aeronaut.*, vol. 34, no. 4, pp. 265–278, 2021.

[29] J. W. Betz and K. R. Kolodziejski, "Extended theory of early-late code tracking for a bandlimited GPS receiver," *Navigation*, vol. 47, no. 3, pp. 211–226, 2000.

[30] J. W. Betz, "Design and performance of code tracking for the GPS M code signal," in *Proc. 13th Int. Tech. Meeting Satell. Division Inst. Navigat. (ION GPS)*, Salt Lake City, UT, USA, Sep. 2000, pp. 2140–2150.

[31] E. S. Lohan, "Analytical performance of CBOC-modulated galileo E1 signal using sine BOC(1,1) receiver for mass-market applications," in *Proc. IEEE/ION Position Location Navig. Symp.*, 2010, pp. 245–253.

[32] E. D. Kaplan and C. J. Hegarty, Eds., *Understanding GPS: Principles and Applications*, 2nd ed. New York, NY, USA: Artech House, 2006.

[33] G. Dai, X. Chen, M. Wang, E. Fernández, T. N. Nguyen, and G. Reinelt, "Analysis of satellite constellations for the continuous coverage of ground regions," *J. Spacecraft Rockets*, vol. 54, no. 6, pp. 1294–1303, Nov. 2017.

[34] J. Wertz *et al.*, *Mission Geometry: Orbit and Constellation Design and Management: Spacecraft Orbit and Attitude Systems* (Space Technology Library). New York, NY, USA: Microcosm, 2001, p. 726.

[35] S. Jaeckel, L. Raschkowski, K. Börner, and L. Thiele, "QuaDRiGa: A 3-D multi-cell channel model with time evolution for enabling virtual field trials," *IEEE Trans. Antennas Propag.*, vol. 62, no. 6, pp. 3242–3256, Jun. 2014.

[36] S. Jaeckel, L. Raschkowski, K. Borner, L. Thiele, F. Burkhardt, and E. Eberlein, *QuaDRiGa—Quasi Deterministic Radio Channel Generator, User Manual and Documentation*, Fraunhofer Heinrich Hertz Inst., Berlin, Germany, 2014.

[37] S. Jaeckel, L. Raschkowski, and L. Thieley, "A 5G-NR satellite extension for the QuaDRiGa channel model," in *Proc. Joint Eur. Conf. Netw. Commun. 6G Summit (EuCNC/6G Summit)*, 2022, pp. 142–147, doi: 10.1109/EuCNC/6GSummit54941.2022.9815679.

[38] S. W. Paek, S. Balasubramanian, S. Kim, and O. de Weck, "Small-satellite synthetic aperture radar for continuous global Biospheric monitoring: A review," *Remote Sens.*, vol. 12, no. 16, p. 2546, 2020.

[39] P. Steigenberger, S. Thoelert, and O. Montenbruck, "GNSS satellite transmit power and its impact on orbit determination," *J. Geodesy*, vol. 92, no. 6, pp. 609–624, Jun. 2018.

[40] Starlink. "SPACEX Non-Geostationary Satellite System, Attachment A: Technical Information to Supplement Schedule." 2020. Accessed: Nov. 19, 2021. [Online]. Available: https://fcc.report/IBFS/SAT-MOD-20181108-00083/1569860.pdf

[41] Oneweb. "ONEWEB Non-Geostationary Satellite System (LEO) Phase 2: Modification to Authorized System." 2020. Accessed: Nov. 10, 2021. [Online]. Available: https://fcc.report/IBFS/SAT-MPL-20200526-00062/2379706.pdf

[42] K. S. LLC. "Application of Kuiper Systems LLC for Authority to Launch and Operate a Non-Geostationary Satellite Orbit System in Ka-Band Frequencies: Technical Appendix." 2021. Accessed: Nov. 15, 2021. [Online]. Available: https://apps.fcc.gov/els/GetAtt.html?id=285359&x=

[43] S. M. Kay, *Fundamentals of Statistical Signal Processing: Estimation Theory*. Upper Saddle River, NJ, USA: Prentice Hall, 1997.

[44] L. G. Jacchia, "Thermospheric temperature, density, and composition: New models," Smithsonian Astrophys. Observatory (SAO), Cambridge, MA, USA, SAO Special Rep. 375, Mar. 1977.

[45] A. E. Hedin, "MSIS-86 thermospheric model," *J. Geophys. Res. Space Phys.*, vol. 92, no. A5, pp. 4649–4662, 1987.

**Jaan Praks** (Senior Member, IEEE) received the B.Sc. degree in physics from the University of Tartu, Tartu, Estonia, in 1996, and the D.Sc. (Tech.) degree in space technology and remote sensing from Aalto University, Espoo, Finland, in 2012.

He is an Assistant Professor of Electrical Engineering with the Department of Electronics and Nanoengineering, School of Electrical Engineering, Aalto University. He has been working with microwave remote sensing, scattering modeling, microwave radiometry, hyperspectral imaging, and advanced SAR techniques, such as polarimetry, interferometry, polarimetric interferometry, and tomography. One of the most visited topics in his research is remote sensing of boreal forest. Since 2009, he has taken an interest in emerging nanosatellite technology. He led a project which produced two of the first Finnish satellites. He has been involved also in spinning off several companies in the field of satellite remote sensing. His research team is a member of the Finnish Centre of Excellence in Research of Sustainable Space and he is a Principal Investigator of several small satellite missions.

Dr. Praks is an Active Member of the scientific community, a member of the Finnish National Committee of COSPAR, the Chairman of the Finnish National Committee of URSI, and the chair/co-chair of many national and international conferences.

**Gonzalo Seco-Granados** (Senior Member, IEEE) received the Ph.D. degree in telecommunications engineering from the Universitat Politecnica de Catalunya, Barcelona, Spain, in 2000, and the M.B.A. degree from IESE Business School, Barcelona, in 2002.

From 2002 to 2005, he was a member of the European Space Agency, Paris, France, where he was involved in the design of the Galileo system and receivers. In 2015 and 2019, he was a Fulbright Visiting Scholar with the University of California at Irvine, Irvine, CA, USA. He is currently a Professor with the Department of Telecommunication, Universitat Autònoma de Barcelona, Barcelona, where he has served as the Vice Dean of the Engineering School from 2011 to 2019. His research interests include statistical signal processing with application to GNSS and 5G localization.

Prof. Seco-Granados has been serving as a member of the Sensor Array and Multi-Channel Technical Committee for the IEEE Signal Processing Society since 2018. He has been the President of the Spanish Chapter of the IEEE Aerospace and Electronic Systems Society since 2019.

**Ruben Morales Ferre** (Student Member, IEEE) received the B.Sc. degree in telecommunication systems engineering and the M.Sc. degree in telecommunication engineering from the Universitat Autònoma de Barcelona (UAB), Barcelona, Spain, in 2016 and 2018, respectively. He is currently pursuing a double Ph.D. degree with Tampere University (TAU), Tampere, Finland, and UAB.

He worked as a Research Assistant with the Signal Processing for Communications and Navigation Group, UAB, until 2018. In 2018, he received a TAU Rector's Grant, which partially finances his Ph.D. studies. He is also involved as a Ph.D. Researcher in EU and Academy of Finland funded projects. His current research interests include GNSS security and integrity, signal processing with applications to communications and navigation, and positioning by means of GNSS and alternative positioning methods, such as cellular networks or LEO constellations, and array signal processing.

**Elena Simona Lohan** (Senior Member, IEEE) received the M.Sc. degree in electrical engineering from the Polytechnic University of Bucharest, Bucharest, Romania, in 1997, the D.E.A. degree (French equivalent of master) in econometrics from the Ecole Polytechnique, Paris, France, in 1998, and the Ph.D. degree in telecommunications from the Tampere University of Technology, Tampere, Finland, in 2003.

She is currently a Professor with the Electrical Engineering Unit, Tampere University, Tampere, and the Coordinator of the MSCA EU A-WEAR Network. Her current research interests include wireless location techniques, wearable computing, and privacy-aware positioning solutions.